1.56 μm and 2.86 μm Raman lasers based on gas-filled anti-resonance hollow-core fiber

Wei Huang (黄 威)[1], Yulong Cui (崔宇龙)[1], Zhixian Li (李智贤)[1], Zhiyue Zhou (周智越)[1], and Zefeng Wang (王泽锋)[1,2,3,*]

[1]*College of Advanced Interdisciplinary Studies, National University of Defense Technology, Changsha 410073, China*
[2]*State Key Laboratory of Pulsed Power Laser Technology, Changsha 410073, China*
[3]*Hunan Provincial Key Laboratory of High Energy Laser Technology, Changsha 410073, China*
**Corresponding author: zefengwang_nudt@163.com*

Received February 15, 2019; accepted April 12, 2019; posted online July 1, 2019

We report here a single-pass 1.56 μm fiber gas Raman laser in a deuterium-filled hollow-core fiber and a 2.86 μm cascade fiber gas Raman laser with methane in the second stage. The maximum output powers at 1.56 and 2.86 μm are 27 and 8.5 mW with Raman conversion efficiency of 30% and 42%, respectively. The results offer a new method to produce a 1.5 μm fiber source and prove the potential of the cascade fiber gas Raman laser in extending the available wavelength.

OCIS codes: 140.3280, 140.3510, 140.3550, 140.4130.
doi: 10.3788/COL201917.071406.

Fiber lasers with high conversion efficiency, efficient heat dissipation, high beam quality, and compact configuration have been widely used in many aspects[1–4]. However, due to the limitations of nonlinear effects, low damage threshold, and transmission bands, silica glass fibers have difficulties in generating narrow linewidth lasers with high peak power, especially at long wavelengths[2]. Since first demonstrated in 1963[5], gas stimulated Raman scattering (SRS) has proven to be an effective method of generating new wavelength lasers, especially in the ultraviolet and mid-infrared ranges[6,7], but the short interaction length and usual generation of high-order Stokes waves result in the high threshold and low conversion efficiency to a single-wavelength Stokes wave with traditional gas cells. The advent of hollow-core fibers (HCFs) with low loss offers an alternative method in solving the problems mentioned above. In HCFs, the light beam can be confined in a small core, providing very strong pump intensity along a very long interaction length. In addition, the transmission bands of HCFs can be easily designed with the pump and the wanted Stokes wavelengths within the transmission bands and the unwanted Stokes in high-loss bands, making it possible to generate efficient Raman conversion to a single wanted Stokes wave in a single-pass structure.

Since first demonstrated in 2002[8], SRS in a gas-filled HCF has attracted enormous attention[9–20]. In 2017, we first reported a 1.5 μm ultra-efficient Raman amplifier in methane-filled negative curvature HCF with a near quantum-limit efficiency of 96.3%[14]. In 2018, Gladyshev *et al.* reported 2.9, 3.3, 3.5 μm Raman lasers based on a revolver-type HCF filled by a mixture of H_2 and D_2, and the quantum conversion efficiency was ∼10%[17]. In the same year, Cao *et al.* reported a 2.8 μm second vibrational Stokes wave through the SRS of methane gas in one methane-filled nodeless HCF, and the maximum quantum efficiency from the pump to the second Stokes wave was ∼40%[18]. Later, we reported a 2.8 μm Raman source in two independent methane-filled HCFs, achieving a total quantum efficiency of ∼65% from 1 to 2.8 μm[19]. In 2019, Astapovich *et al.* reported a 4.42 μm Raman laser with an average output of 1.4 W and a quantum efficiency of 53%, through the Raman effect of H_2 pumped by a 1.5 μm erbium-doped fiber laser[20]. Up to now, there are no reports on SRS in only deuterium-filled HCFs, which can generate a longer wavelength laser in the 1.5 μm band than ethane[13]and methane[14] and can arrive at a longer wavelength in mid-infrared ranges by cascaded SRS with other gases[19].

In this Letter, we have for the first time, to the best of our knowledge, investigated the characteristics of the SRS of deuterium gas in an HCF. By using a high peak power 1064.6 nm laser as the pump source, we obtain the Stokes output at 1560.9 nm with a Raman conversion efficiency of 30%. By adjusting the deuterium pressure, the maximum output power of the SRS of D_2 is achieved, which is then coupled into another HCF filled with methane as the pump source, and we obtain 8.5 mW Stokes output of 2865.5 nm with the conversion efficiency of ∼42%. Combined with our previous work[19], this Letter effectively proves the potential of this kind of cascade HCF Raman laser in extending wavelengths.

The experimental setup is shown in Fig. 1, which is similar to the setup of our previous work[19]. The setup consists of two stages. In the first stage, HCF1 is filled with deuterium gas and is pumped with a 1064.6 nm pulse microchip laser (linewidth of ∼6 pm, pulse duration of ∼1.5 ns, repetition rate of 1 kHz, and average power of ∼160 mW). The pump light is coupled into HCF1 through a telescope system consisting of two convex-plane lenses. A combination of a $\lambda/2$ plate and a polarization beam splitter (PBS) is employed to adjust the incident pump power. Another $\lambda/2$ plate set after the PBS is used to adjust the

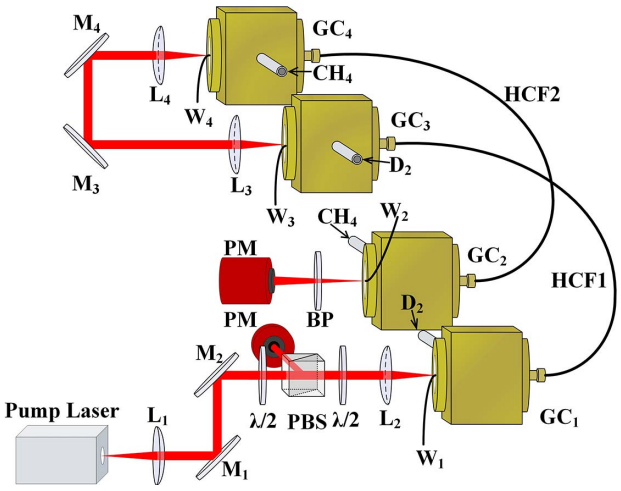

Fig. 1. Experimental setup: M, coated high-reflection mirror; $\lambda/2$, half-wave plate; PBS, polarization beam splitter; L, convex-plane lens; W, anti-reflection coated window with high transmission rate; GC, gas cell; PM, power meter; BP, band-pass filter.

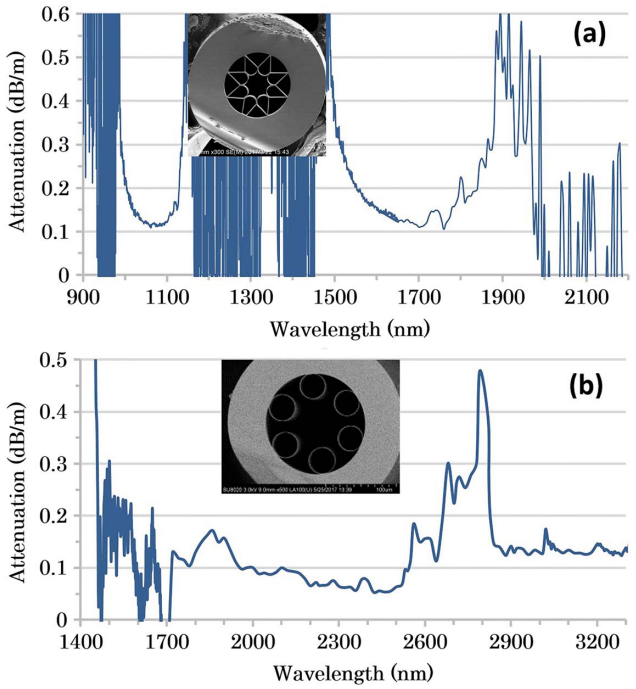

Fig. 2. Transmission spectra of (a) HCF1 and (b) HCF2 measured with the cut-off method. Insets: the scanning electron micrographs of the HCFs' cross sections.

polarization so as to optimize the coupling efficiency, as the HCF is slightly polarization-dependent. In the second stage, HCF2 is filled with methane gas, and the 1560.9 nm Stokes light from HCF1 is collimated and coupled into HCF2 through a similar telescope system. A filter (Thorlabs FB2750-500, transmission ~75% at 2865.5 nm and attenuation >40 dB at 1560.9 nm) placed after the output window of gas cell 2 is used to remove the residual 1064.6 and 1560.9 nm power, just leaving the 2865.5 nm Stokes wave for measurements.

The HCFs used in the experiment are the same as that used in our previous work[19], whose transmission spectra are shown in the Figs. 2(a) and 2(b). The losses at 1.06 and 1.56 μm are 0.12 and 0.2 dB/m for HCF1 in the first stage. The losses at 1.56 and 2.8 μm are 0.18 and 0.14 dB/m for HCF2 in the second stage. The cross sections of the two HCFs used in our experiments are inserted in Figs. 2(a) and 2(b) with core diameters of ~46 and ~75 μm.

Figure 3 shows the measured output spectrum in the first stage for a 2 m fiber at 4, 6, and 10 bar (1 bar = 0.1 MPa) pressure with 50 and 90 mW coupled pump power. The spectrum is recorded by two optical spectrum analyzers (OSAs, Yokogawa, Japan, AQ6370D, range of 600–1700 nm and AQ6375B, range of 1200–2400 nm). The change of the noise level at 1200 nm is due to change of the OSAs, so the relative intensities should be taken only as indicative. It can be seen that there are lots of Raman lines in the SRS process of deuterium gas, including vibrational Raman lines [vibrational Stokes (VS1), vibrational anti-Stokes (VAS1, VAS2, VAS3)] and rotational Raman lines scattered around those vibrational lines. The reason is that the Raman gain of rotational SRS of deuterium is numerically similar to that of vibration SRS, which is pretty different from the SRS of methane[14]. In addition, we also observe the rotational SRS of ortho-deuterium (Raman shift of 197 cm^{-1}) under the condition of 10 bar pressure and 90 mW coupled power. We can also see that at 10 bar pressure with 90 mW coupled pump power, even the third-order rotational Stokes (RS) line (VS1 + RS3) of VS1 can be observed, while there is only the first rotational anti-Stokes (RAS) line (VS1 + RAS1) of VS1 in the spectrum, which is because high-order RAS lines are not located in the transmission bands. From the spectrum, we can observe that at 4 bar deuterium pressure, the Raman output includes 1560.9 nm (VS1), 807.5 nm (VAS1), 650.5 nm (VAS2), and 1019.4 nm (RAS1). However, when the pressure increases, the output spectrum covers more rotational Raman lines, which is because Raman gain increases at high pressure, resulting in low thresholds of rotational SRS. Thus, in our experiment, in order to obtain efficient first-order vibrational Stokes light of 1560.9 nm, the pressure is set at 4 bar.

The pulse shapes of the 1064.6 and 1560.9 nm are measured by a fast InGaAs photodetector (EOT ET5000, wavelength ranging from 850 to 2150 nm, bandwidth 12.5 GHz, rise time <28 ps) and a broadband oscilloscope (Tektronix DPO72504DX, bandwidth 25 GHz, sampling rate 100 GSa/s), which are shown in Fig. 4. The pulse duration of the pump and first-order Stokes line is 1.47 and 1.37 ns, respectively. Similar to the SRS of hydrogen or methane in an HCF[13,15,16], the pulse width of a Stokes wave is shorter, and the leading edge is steeper compared with the pump light, because only the part of pump pulse over the threshold can be converted to a Stokes wave, which indicates the pulse compression effect of SRS[21].

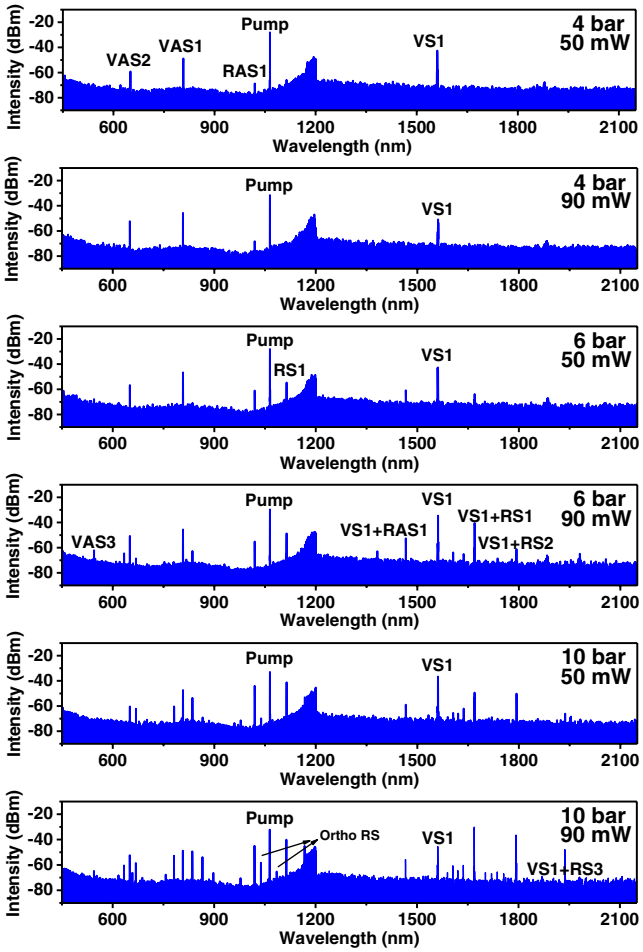

Fig. 3. Measured optical spectra of 2 m deuterium-filled HCFs with different gas pressure and coupled pump power. VS, vibrational Stokes; VAS, vibrational anti-Stokes; RS, rotational Stokes; RAS, rotational anti-Stokes. VS1: 1560.9 nm; VAS1: 807.5 nm; VAS2: 650.5 nm; VAS3: 544.6 nm; RS1: 1113.6 nm; RAS1: 1019.4 nm; VS1 + RS1: 1669 nm; VS1 + RAS1: 1466 nm; VS1 + RS2: 1793 nm; VS1 + RS3: 1937.2 nm. Ortho RS, rotational SRS of ortho deuterium.

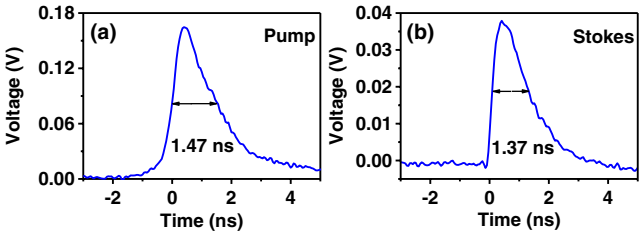

Fig. 4. Measured (a) pump and (b) Stokes pulse shape using a fast detector and a broad bandwidth oscilloscope with a 2 m HCF filled with 4 bar of deuterium gas.

We also measured the exact linewidths of the pump and the VS wave with Fabry–Perot (F–P) interferometers, just as was done in our previous work[13,14]. The linewidth of pump light is about 1.19 GHz, and there is no obvious change when we increase the power. The linewidth of the first VS wave is about 1.27 GHz.

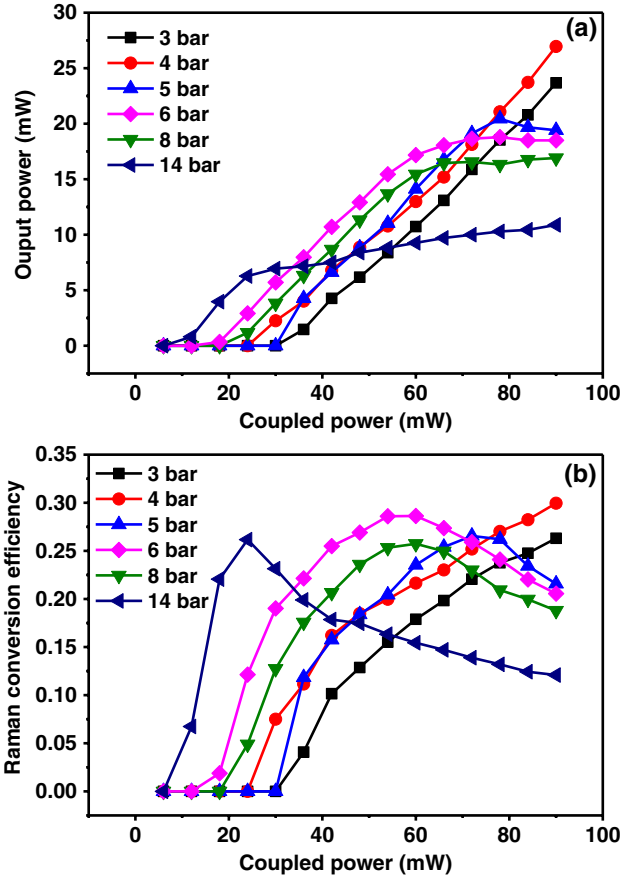

Fig. 5. (a) Output power and (b) Raman conversion efficiency at 1560.9 nm in a 2 m HCF change with incident pump power and deuterium pressure in the first stage.

The output power of the first-order Stokes at 1560.9 nm with different pump power at various pressures is shown in Fig. 5(a). It was measured through a filter (Thorlabs BP1550-40, transmission ~57% at 1560.9 nm and attenuation >30 dB outside the transmission band), which was placed after the output window of gas cell 3 to remove the residual pump light and other Raman lines. The figure shows that with the increase of pressure, the threshold of SRS gradually decreases, which resulted from higher Raman gain at higher pressure. When the pump power exceeds the threshold, the Stokes power increases linearly with the pump power, but at high pressure, the saturation point appears and reduces the power growth. It is because at high pressure, more Raman lines are generated, as shown in Fig. 3, inhibiting the conversion to a 1560.9 nm Stokes wave and increasing the dissipation of it, converting it to other lines. Another reason is that Raman-enhanced self-focusing transfers the energy of the fundamental mode to a higher-order mode, which attenuates rapidly[8]. Therefore, with the increase of pressure, the maximum output power increases first and then decreases, as shown in Fig. 5(a). Figure 5(b) shows the Raman conversion efficiency changes with coupled power at different pressure. It can be seen that at high pressure, the Raman conversion efficiency has a maximum value at the

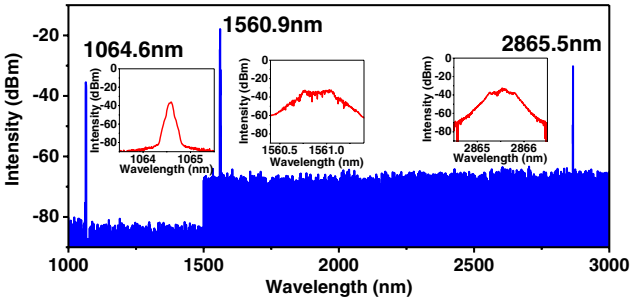

Fig. 6. Measured spectrum of the output of HCF2 in the second stage, measured with 2.2 m fiber length and 12 bar methane pressure. The change of the noise level at 1500 nm is due to the change of the OSAs, so the relative intensities should be taken only as indicative. Inset: measured fine spectrum near 1064.6 nm (left), 1560.9 nm (middle), and 2865.5 nm (right), respectively, with an OSA resolution of 0.02 nm.

saturation point, and at 4 bar pressure, the Raman conversion efficiency achieves the highest. According to the results, the optimum pressure in our experiment in the first stage is 4 bar, giving a maximum average output power of 27 mW (pulse energy of ~27 μJ, peak power of ~20 kW) and Raman conversion efficiency of 30%.

After setting the optimum deuterium pressure (4 bar) to achieve maximum output at 1560.9 nm, we carry out the cascaded experiment of deuterium and methane. The optical spectrum of the output of HCF2 filled with 14 bar methane is shown in Fig. 6, measured with two OSAs (Yokogawa, Japan, AQ6370D, range of 600–1700 nm and AQ6376D, range of 1500–3400 nm). From the spectrum, we can see that there exist only three lines, 1064.6 nm (pump light), 1560.9 nm (first-order Stokes line of deuterium), and 2865.5 nm (first-order Stokes line of methane), while no other lines are observed. Because the Raman scattering coefficient of vibrational SRS of methane is much higher than that of other lines, only 2865.5 nm light can be generated with the pump of the 1560.9 nm Stokes wave[22]. The reason why no Raman signal is generated by 1064.6 nm light is that the residual pump power at 1064.6 nm is low, and its coupling coefficient for HCF2 is also low, as the telescope system in the second stage is set for a 1560.9 nm wave. The measured fine spectrum near 1064.6, 1560.9, and 2865.5 nm is shown as the inset in Fig. 6.

The relationship of measured 2865.5 nm power with the coupled 1560.9 nm power at different methane pressures in the second stage is shown in Fig. 7(a). Similar to the results in the first stage, the 2865.5 nm Stokes power increases linearly with the 1560.9 nm power beyond the threshold. With the increase of the methane pressure, the Raman threshold decreases, and the output power has a maximum value. Figure 7(b) shows the Raman conversion efficiency from 1560.9 to 2865.5 nm at different pressures, coupled with different power. According to our experimental research, in the second stage, the maximum output power at 2865.5 nm is 8.5 mW, obtained at 14 bar, with a Raman conversion efficiency of 41.9%.

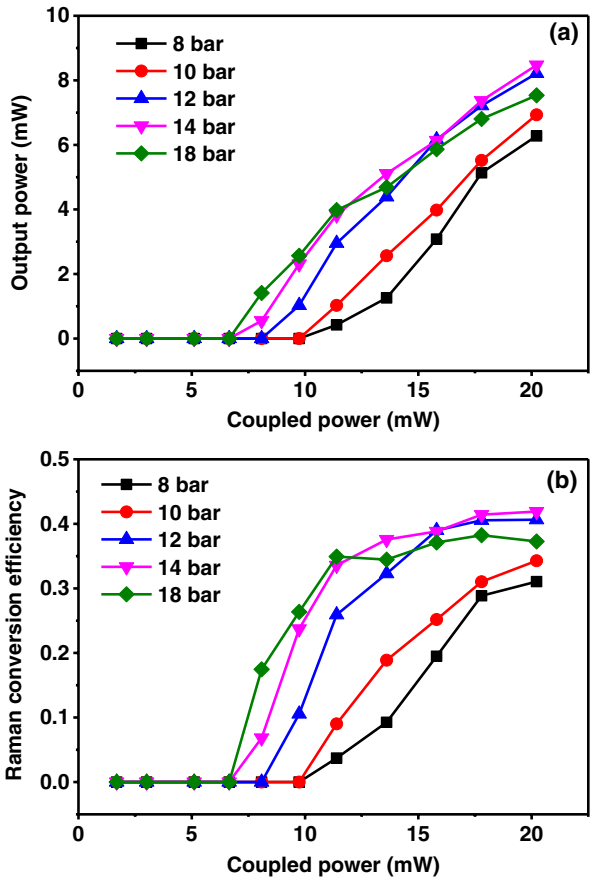

Fig. 7. (a) Output power and (b) Raman conversion efficiency at 2865.5 nm in a 2.2 m HCF changing with incident 1560.9 nm power and methane pressure in the second stage.

In conclusion, we have first, to the best of our knowledge, demonstrated a single-pass deuterium gas Raman fiber laser operating at 1560.9 nm with maximum output of 27 mW, corresponding to the Raman conversion efficiency of 30%. We also report a 2.8 μm cascaded Raman gas fiber laser by letting the deuterium Raman laser be the first stage and a methane Raman laser pumped with the 1560.9 nm output light be the second stage. In the second stage, we have achieved an 8.5 mW maximum output at 2865.5 nm, and the Raman conversion efficiency is 41.9%. This work provides a new opportunity for efficient mid-infrared fiber gas laser sources, which have a wide range of applications in many fields.

This work was partly supported by the Outstanding Youth Science Fund Project of Natural Science Foundation of Hunan Province (No. 19JJ20023) and the National Natural Science Foundation of China (NSFC) (No. 61705266). We are grateful to Professor Jonathan C. Knight from the University of Bath in the UK for providing the HCFs used in the first stage, and we also thank Dr. Yingying Wang from Beijing University of Technology for providing the HCFs used in the second stage of our experiments.

References

1. W. Shi, A. Schulzgen, R. Amezcua, X. Zhu, and S. Alam, J. Opt. Soc. Am. B **34**, FLA1 (2017).
2. S. W. Harun, S. Alam, A. S. Kurkov, M. C. Paul, and Z. Sun, IEEE J. Sel. Top. Quantum Electron. **20**, 5 (2014).
3. Z. Qin, G. Xie, J. Ma, P. Yuan, and L. Qian, Chin. Opt. Lett. **15**, 111402 (2017).
4. S. Vyas, T. Tanabe, M. Tiwari, and G. Singh, Chin. Opt. Lett. **14**, 123201 (2016).
5. R. W. Minck, R. W. Terhune, and W. G. Rado, Appl. Phys. Lett. **3**, 181 (1963).
6. D. J. Brink and D. Proch, Opt. Lett. **7**, 494 (1982).
7. A. D. Papayannis, G. N. Tsikrikas, and A. A. Serafetinides, Appl. Phys. B **67**, 563 (1998).
8. F. Benabid, J. C. Knight, G. Antonopoulos, and P. St. J. Russell, Science **298**, 399 (2002).
9. F. Benabid, G. Antonopoulos, J. C. Knight, and P. St. J. Russel, Phys. Rev. Lett. **95**, 213903 (2005).
10. F. Couny, F. Benabid, and P. S. Light, Phys. Rev. Lett. **99**, 143903 (2007).
11. F. Couny, in *Conference on Lasers and Electro-Optics* (2010), paper CTuM3.
12. Z. Wang, F. Yu, W. J. Wadsworth, and J. C. Knight, Laser Phys. Lett. **11**, 105807 (2014).
13. Y. Chen, Z. Wang, B. Gu, F. Yu, and Q. Liu, Opt. Lett. **41**, 5118 (2016).
14. Y. Chen, Z. Wang, Z. Li, W. Huang, X. Xi, and Q. Lu, Opt. Express **25**, 20944 (2017).
15. Z. Wang, B. Gu, Y. Chen, Z. Li, and X. Xi, Appl. Opt. **56**, 7657 (2017).
16. Z. Li, W. Huang, Y. Cui, and Z. Wang, Appl. Opt. **57**, 3902 (2018).
17. A. V. Gladyshev, A. F. Kosolapov, M. M. Khudyakov, Y. P. Yatsenko, A. N. Kolyadin, A. A. Krylov, A. D. Pryamikov, A. S. Biriukov, M. E. Likhachev, I. A. Bufetov, and E. M. Dianov, IEEE J. Sel. Top. Quantum Electron. **24**, 0903008 (2018).
18. L. Cao, S. Gao, Z. Peng, X. Wang, Y. Wang, and P. Wang, Opt. Express **26**, 5609 (2018).
19. Z. Li, W. Huang, Y. Cui, and Z. Wang, Opt. Lett. **43**, 4671 (2018).
20. M. S. Astapovich, A. V. Gladyshev, M. M. Khudyakov, A. F. Kosolapov, M. E. Likhachev, and I. A. Bufetov, IEEE Photon. Technol. Lett. **31**, 78 (2019).
21. R. L. Carman, F. Shimizu, C. S. Wang, and N. Bloembergen, Phys. Rev. A **2**, 60 (1970).
22. S. Montero and D. Bermejo, Mol. Phys. **32**, 1229 (1976).